ANATOMIA HISTOLOGIA EMBRYOLOGIA
JOURNAL OF VETERINARY MEDICINE

Anat. Histol. Embryol. **38,** 18–22 (2009)
ISSN 0340–2096

doi: 10.1111/j.1439-0264.2008.00886.x

Departamento de Morfología (Anatomía y Embriología), Facultad de Veterinaria, Universidad de Las Palmas de Gran Canaria, Las Palmas de Gran Canaria, Spain

CT-Soft Tissue Window of the Cranial Abdomen in Clinically Normal Dogs: An Anatomical description using Macroscopic Cross-Sections with Vascular Injection

M. A. Rivero[1]*, J. M. Vázquez[2], F. Gil[2], J. A. Ramírez[1], J. M. Vilar[3], A. De Miguel[1] and A. Arencibia[1]

Addresses of authors: [1]Department of Morphology, Faculty of Veterinary, University of Las Palmas de Gran Canaria, 35416 Las Palmas de Gran Canaria; [2]Department of Anatomy, Faculty of Veterinary, University of Murcia, 30100 Murcia; [3]Department of Pathology, Faculty of Veterinary, University of Las Palmas de Gran Canaria, 35416 Las Palmas de Gran Canaria, Spain; *Corresponding author: Tel.: 0034928454352; fax: 0034928451141; e-mail: mrivero@dmor.ulpgc.es

With 5 figures

Received October 2007; accepted for publication June 2008

Summary

The aim of this study was to provide a detailed anatomic atlas of the cranial abdomen by means of computed tomography (CT). Three mature dogs, all mixed breed males, were used. The dogs were sedated, anaesthetized and positioned in sternal recumbency. CT scans from the eighth thoracic vertebra to the fourth lumbar vertebra were performed using a third-generation equipment (TOSHIBA 600HQ scanner) with 1 cm slice thickness. CT-images of the cranial abdomen were taken with soft-tissue window (WL: −14, WW: 658) settings. Dogs were killed and vascular-injection technique was performed: red and blue latex filled the vascular system. Injected dogs were frozen in the same position as used for CT examination and sectioned with an electric bandsaw at 1-cm-thick intervals. The cuts matched as closely as possible to the CT-images. The anatomic sections were compared and studied with the corresponding CT-images, and clinically relevant abdominal anatomic structures were identified and labelled on the corresponding CT-images. The results of our study could be used as a reference for evaluating CT-images of the canine cranial abdomen with abdominal diseases.

Introduction

During the last two decades, computed tomography (CT) of the corporal cavities has been established as an important and useful imaging modality in veterinary medicine (Samii et al., 1998). An increasing number of reports in different journals or books are found involving thoracic and abdominal CT (Feeney et al., 1991; Smallwood and George, 1993; Assheuer and Sager, 1997; Samii et al., 1998; De Rycke et al., 2005; Rivero et al., 2005; Teixeira et al., 2007). In human medicine, CT has become the imaging technique of choice for the diagnosis (Novelline et al., 1999) and evaluation of various abdominal syndromes and disorders such as primary or metastatic neoplasia (Ri-Sheng et al., 2006), renal calculus (Girgin et al., 2007), injury in vessels (Schwartz et al., 2007) and liver abscess (Syed et al., 2007).

CT provides, in a transversal plane, excellent diagnostic information that is unobtainable with conventional radiographic techniques (De Rycke et al., 2005). This is because of a better distinction among the different CT tissue densities in the abdominal cavity (Fike et al., 1980; Stickle and Hathcock, 1993). Accurate interpretation and identification of CT-images require a thorough knowledge of the planimetric anatomy and its topography (Feeney et al., 1991; Smallwood and George, 1993; Samii et al., 1998). Although other authors have addressed cross-sectional anatomy of the abdomen using CT and other techniques (Feeney et al., 1991; Smallwood and George, 1993; Assheuer and Sager, 1997), we believe that our work includes additional information such as adding better quality CT-images and comparing them with anatomical specimens that have been vascularly injected for a better definition of the morphology and topography of the vascular structures. The purpose of this study was to provide a colour atlas of the canine cranial abdomen by means of gross anatomic sections compared with their corresponding CT-images.

Materials and Methods

Three mature dogs, all mixed breed males, were used for this study. Their weight ranged from 25 to 34 kg and their average height was 60 cm. The dogs were sedated with 0.2 mg/kg acepromazine (Calmo Neosan; Pfizer, New York, NY, USA) and anaesthetized with 15 mg/kg intravenous sodium pentobarbital (Braun; Braun Medical, Melsungen, Germany). Throughout the procedure, the animals were maintained in sternal recumbency perpendicular to the exploration table. The CT-study was performed at the Radiodiagnostic Service of the Hospital Universitario Insular of Las Palmas de Gran Canaria with a TOSHIBA 600HQ scanner (third generation equipment; Toshiba Medical Imaging Systems, Tustin, CA, USA). Transverse slices from the eighth thoracic vertebra to the fourth lumbar vertebra were obtained using the following parameters: caudal vision of image (V.V.F.), 8 s exposure time, 120 kV, 80 mA, 1 cm slice thickness. Best image quality for soft tissue was obtained by adjusting window widths and window levels. For soft tissue abdominal structures, a soft-tissue window was used (WL: −14, WW: 658).

Immediately following the CT study, the dogs were killed using a sodium pentobarbital overdose. The dogs were exsanguinated with a 0.9% saline solution and latex was injected into their arterial and venous systems: A red latex injection into the left common carotid artery filled the systemic

arteries and the pulmonary veins, whereas a blue latex injection into the left external jugular vein filled the systemic veins and the pulmonary arteries. As a result, the blood vessels were clearly identified, except the portal system of veins in which the latex could not perfuse.

To minimize post-mortem changes, the injected dogs were frozen within 24 h at −70°C in the same position as they were scanned. Once the cadavers were completely frozen, they were sectioned with an electric bandsaw at the positions which matched the CT-images as closely as possible. Each section was 1 cm thick. Sections were carefully cleaned with water and their caudal surfaces were photographed. Anatomical atlases (Feeney et al., 1991; Ruberte et al., 1998; Vázquez et al., 2000) were used to identify the structures of the cranial abdomen and correlated to analogous structures on the CT-images. Illustrated veterinary anatomical nomenclature (Schaller, 1992) was used in accordance with official anatomic terminology. Although CT and cross-section have approximately the same slice position and orientation, some structures labelled in the anatomic cross-section could not be identified in its corresponding CT-images.

Results

Clinically relevant abdominal anatomic structures were identified and labelled in each of the two photographs presented in the figures (Figs 2–5): CT (a) and anatomic section (b). Figure 1 is a ventrodorsal radiographic image in which the lines depict the CT transverse imaging planes and gross sections (Figs 2–5). These four sections were selected from different dogs and are presented in a cranial to caudal progression from the level of the ninth thoracic vertebra (Fig. 2) to the level of the first lumbar vertebra (Fig. 5). CT-images and anatomic sections were orientated so that the left side of the abdominal cavity is to the viewer's left and dorsal is at the top.

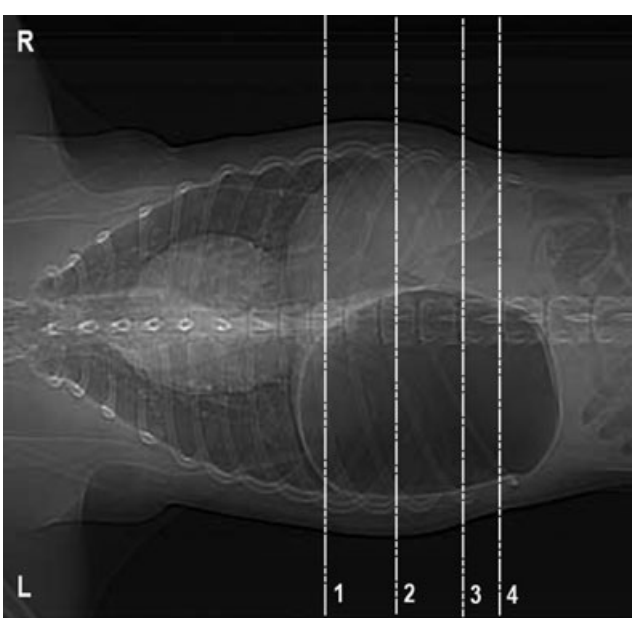

Fig. 1. Ventrodorsal (VD) radiographic image corresponding to thoracic and abdominal regions. Transverse sections (1–4) are shown.

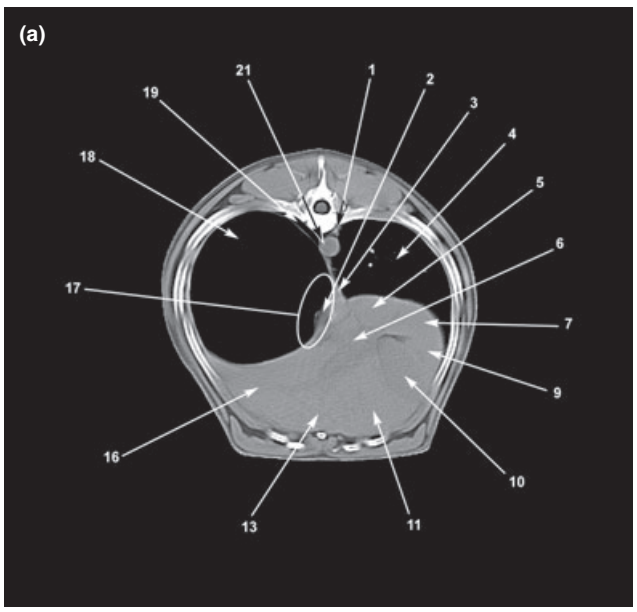

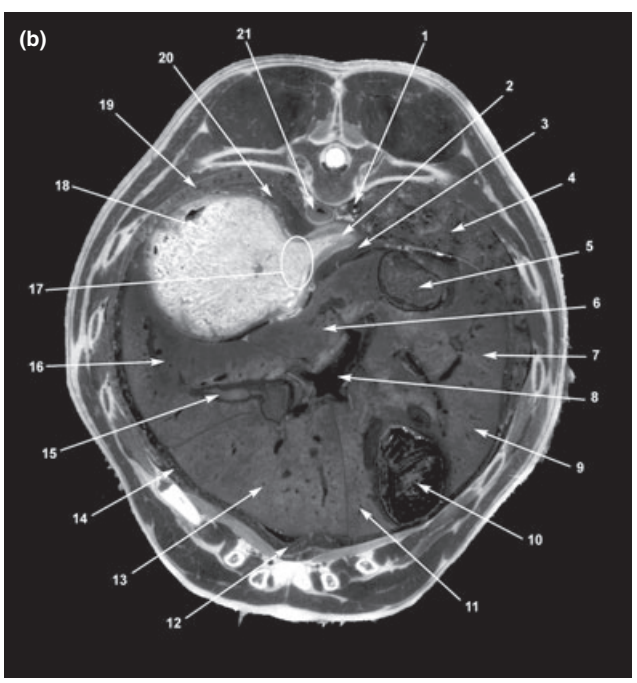

Fig. 2. (a) Transversal computed tomography (CT) scan and (b) anatomical section of the cranial abdomen at the level between 9th and 10th thoracic vertebra. Caudal view (WL: −14, WW: 658). 1, right azygous vein; 2, oesophagus: abdominal part; 3, diaphragm: right crus; 4, right lung: caudal lobe; 5, caudal vena cava; 6, liver: papillary process of caudate lobe; 7, liver: right lateral lobe; 8, portal vein (only b); 9, liver: right medial lobe; 10, gallbladder; 11, liver: quadrate lobe; 12, diaphragm: sternal portion (only b); 13, liver: left medial lobe; 14, diaphragm: costal portion (only b); 15, hepatic veins (only b); 16, liver: left lateral lobe; 17, cardia of stomach; 18, fundus of stomach; 19, left lung: caudal lobe; 20, diaphragm: left crus (only b); 21, descending aorta.

Detailed anatomy of the cranial abdomen was acquired with a soft-tissue window. Grey scale CT is directly related to the radiation attenuation of the abdominal structures. The CT-images provide a good depiction of bone structures. Thus, the walls and the roof bones of the thoracic and abdominal

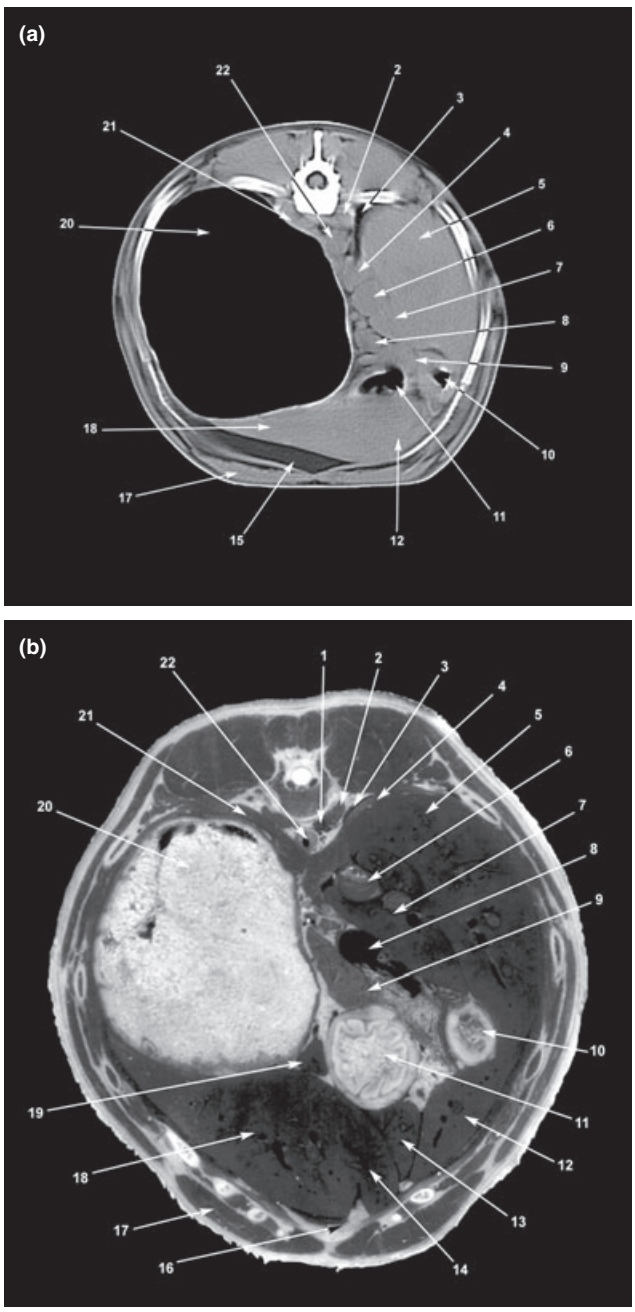

Fig. 3. (a) Transversal computed tomography (CT) scan and (b) anatomical section of the cranial abdomen at the level between 11th and 12th thoracic vertebra. Caudal view (WL: −14, WW: 658). 1, right azygous vein (only b); 2, sublumbar muscles; 3, right pleural cavity; 4, diaphragm: right crus; 5, liver: right lateral lobe; 6, caudal vena cava; 7, liver: caudate process of caudate lobe; 8, portal vein; 9, lesser omentum and pancreas; 10, duodenum: cranial part; 11, pyloric part of stomach; 12, liver: right medial lobe; 13, liver: quadrate lobe (only b); 14, liver: left medial lobe (only b); 15, greater omentum (only a); 16, falciform ligament (only b); 17, m. rectus abdominis; 18, liver: left lateral lobe; 19, liver: papillary process of caudate lobe (only b); 20, fundus of stomach; 21, diaphragm: left crus; 22, descending aorta.

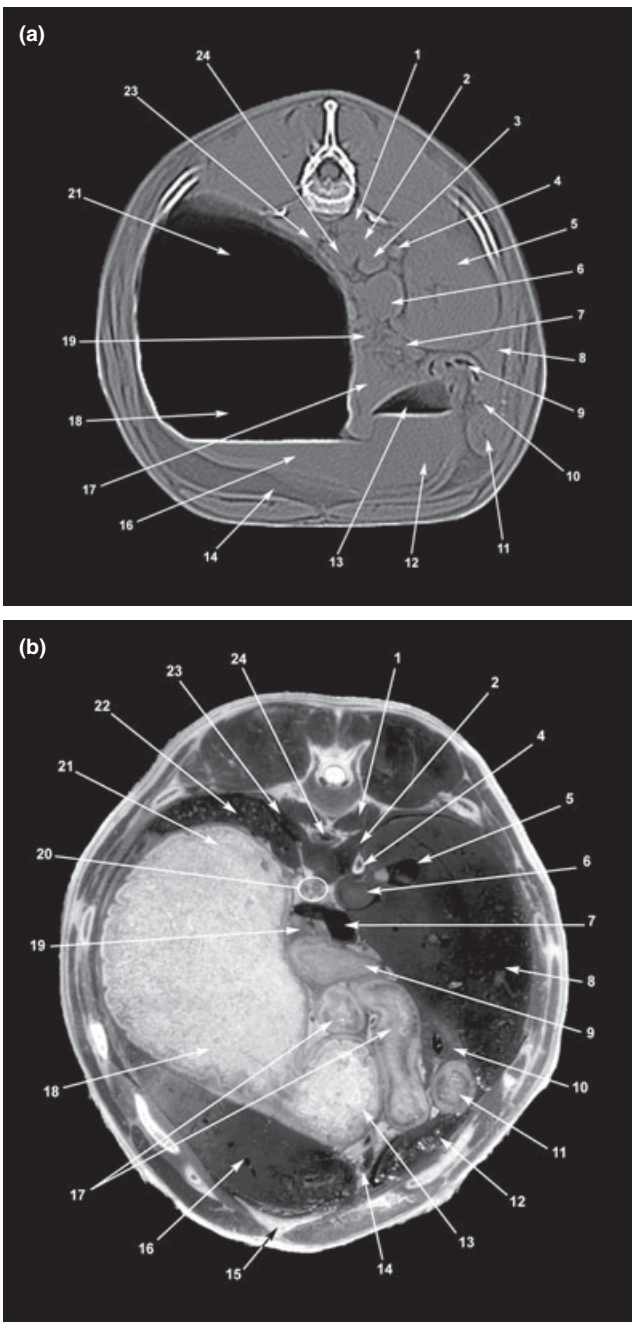

Fig. 4. (a) Transversal computed tomography (CT) scan and (b) anatomical section of the cranial abdomen at the level between 13th thoracic vertebra and first lumbar vertebra. Caudal view (WL: −14, WW: 658). 1, sublumbar muscles; 2, diaphragm: right crus; 3, right renal vein (only a); 4, right adrenal gland; 5, right kidney and caudate process of caudate lobe of the liver; 6, caudal vena cava; 7, portal vein; 8, liver: right lateral lobe; 9, transverse colon; 10, pancreas: right lobe; 11, duodenum: descending part; 12, liver: right medial lobe; 13, pyloric part of stomach; 14, greater omentum; 15, falciform ligament (only b); 16, liver: left lateral lobe; 17, jejunum; 18, body of stomach; 19, lesser omentum and left lobe of the pancreas; 20, Left gastric and hepatic arteries (only b); 21, fundus of stomach; 22, spleen (only b); 23, diaphragm: left crus; 24, descending aorta.

cavities (caudal ribs with their head and tubercle; thoracic and lumbar vertebra with their articular, transverse and spinous processes, vertebral arch and vertebral body) and the sternum (sternebrae and xiphoid process) were easily identifiable because of the high CT-density and appeared white. In the same way, CT-images provided an excellent view of the joint surfaces of the costovertebral, costochondral and sternocostal joints.

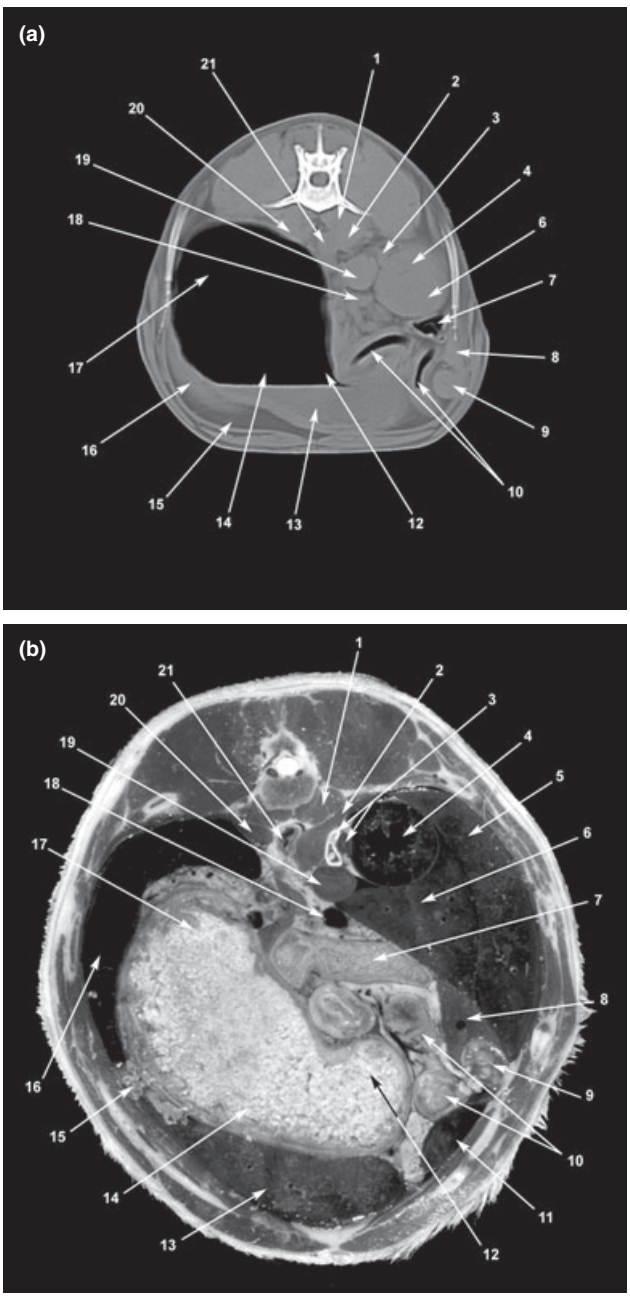

Fig. 5. (a) Transversal computed tomography (CT) scan and (b) anatomical section of the cranial abdomen at the 1st lumbar vertebra. Caudal view (WL: −14, WW: 658). 1, sublumbar muscles; 2, diaphragm: right crus; 3, right adrenal gland and renal vein; 4, right kidney; 5, liver: right lateral lobe (only b); 6, liver: caudate process of caudate lobe; 7, ascending colon; 8, pancreas: right lobe; 9, duodenum: descending part; 10, jejunum; 11, liver: right medial lobe (only b); 12, pyloric part of stomach; 13, liver: left lateral lobe; 14, body of stomach; 15, greater omentum; 16, spleen; 17, fundus of stomach; 18, portal vein; 19, caudal vena cava; 20, diaphragm: left crus; 21, descending aorta.

Figure 2 shows the diaphragmatic crura with an intermediate CT-density and appears grey. The caudal lobe of both lungs appears black with a low opacity compared with the bronchial cartilages, which are observed with an intermediate tissue density. The wall of the stomach is observed grey but its lumen has a low CT-density because it is filled with air. The external contour of the liver is visible and the contour of the gallbladder can discern on the surface of the hepatic parenchyma. Descending aorta, right azygous vein and caudal vena cava are observed grey because they have an intermediate tissue density.

In a more caudal cutting plane (Fig. 3), we visualize different muscles and tendinous structures (diaphragmatic crura, sublumbar muscles and musculus rectus abdominis) with an intermediate tissue density. The right pleural cavity and the lumen of the stomach (fundus and pyloric part) and the cranial part of the duodenum are observed with a low CT-density. Vascular structures (descending aorta, caudal vena cava and portal vein), the liver and the pancreas have an intermediate tissue density compared with the lesser and greater omenta that appear dark grey with a low-intermediate CT-density because they contain adipose tissue.

In Fig. 4, we observe several structures of the digestive system whose wall appears grey but the lumen of the stomach, small intestine (descending part of the duodenum) and large intestine (transverse colon) have a low CT-density. The spleen, the right adrenal gland, the pancreas and the external contour of the right kidney with the caudate process of the caudate lobe of the liver are visualized grey in the abdominal cavity.

In the last figure (Fig. 5), the lumen of the small intestine (descending part of the duodenum, jejunum) and the large intestine (ascending colon) are visualized black because of their low tissue density. Vascular structures (descending aorta and caudal vena cava) and different abdominal organs (liver, right kidney, right adrenal gland and pancreas) are observed with an intermediate CT-density. Finally, some portions of the lesser and greater omenta are observed dark grey.

Discussion

The use of CT as a non-invasive cross-sectional diagnostic imaging technique offers considerable advantages compared with traditional radiography and ultrasound for the examination of the abdominal cavity. Radiographic exploration of the canine abdomen is difficult because of its complex anatomy and individual ultrasound images represent only a portion of the complete cross-sectional anatomy for any level of the body (Samii et al., 1998). CT produces high-detail anatomical images with good soft tissue contrast of the abdomen (Samii et al., 1998). Inferior quality images can be manipulated using the grey scale (Rivero et al., 2005). CT is more sensitive in detecting diseases, and distinguishes normal and abnormal structures accurately (Hounsfield, 1973; Collard et al., 1975; Barbee and Allen, 1987; Thrall, 1994; Ottesen and Moe, 1998). CT imaging studies can provide additional information in patients with radiographic and ultrasonographic patterns of abdominal disorders (Drost, 2003).

As a result of the high costs of the equipment and the anaesthetic risks, abdominal CT is not yet used routinely in veterinary medicine (De Rycke et al., 2005). At times, the anaesthetic risk and diagnostic gain have to be balanced before deciding whether or not to perform a scan (Schwarz, 2003), and an adequate positioning of the patient is important to ensure a good result and anatomic symmetry of the abdominal structures.

CT-exploration takes a relatively long time and therefore involves high radiation dosage. It has been claimed that CT-scanning probably involves the highest radiation exposure

per examination in the field of radiology (Ottesen and Moe, 1998). Recently, this problem has been reduced by means of the use of spiral CT, already used in other abdominal studies (Teixeira et al., 2007). This technique reduced the scan time, resulting in improved temporal resolution and reduced anaesthetic time (Teixeira et al., 2007).

Anatomical structures of the abdomen were evaluated using soft tissue window settings. Window settings should be chosen based on the tissue type to be examined (Schwarz, 2003). CT soft tissue window and cross-sections allow good differentiation between soft tissues of the abdomen. The planimetric or sectional anatomy of the canine abdomen with vascular injection allows a correct morphology and topographic evaluation of the anatomic structures, especially of the systemic veins and arteries, which is a useful tool for the identification of the CT-images. In this study, we have not used intravenous contrast medium because the aim was to describe plain CT-images by standard procedures.

Although the use of CT-imaging in small animal medicine is currently still limited because of its costs and availability, and the logistic problems of acquiring CT-images, CT-imaging for pets becomes more available with developing technology. In the same way, we consider it quite useful to be able to establish some anatomic references on the cranial abdomen, to scan only selected parts during clinical or experimental applications. During the last decade, several works in dogs about the anatomy of the abdomen using CT were published (Feeney et al., 1991; Smallwood and George, 1993; Assheuer and Sager, 1997; Teixeira et al., 2007). To our knowledge, none of the published works have applied and compared CT-images with vascular injected anatomical cross sections. Moreover, a high quality image allows a good and easy interpretation of anatomical structures of the abdominal cavity (Rivero et al., 2005).

In conclusion, the results of our study indicate that the use of anatomic sections with vascular injection is helpful for identifying anatomical structures that are visible on CT-images. These provide detailed information of the structures of the canine abdominal cavity compared with conventional diagnostic imaging techniques (ultrasound, conventional radiography, etc.). We hope that this paper could be used as a reference for evaluating CT-images of canine diseases in the cranial abdomen.

References

Assheuer, J., and M. Sager, 1997: Abdomen. In: MRI and CT Atlas of the Dog, 1st edn. Berlin and Oxford: Blackwell Science Ltd.

Barbee, D. D., and J. R. Allen, 1987: Computed tomography in the horse: general principles and clinical applications. Proc. Am. Assoc. Equine Pract. **32,** 483–493.

Collard, M., H. Dupont, and G. Noel, 1975: Ere nouvelle de la neuroradiologie: la tomographie axiale tranverse computérisée-T.A.T.C(Emi-Scanner) et ses indications. J. Radiol. **56,** 453–469.

De Rycke, L., I. Gielen, P. Simoens, and H. Van Bree, 2005: Computed tomography and cross-sectional anatomy of the thorax in clinically normal dogs. Am. J. Vet. Res. **66,** 512–524.

Drost, W. T., 2003: Abdominal computed tomography. In: Proceedings of Western Veterinary Conference: Section Diagnostic Imaging, Las Vegas, Nevada, February 11–14.

Feeney, D., T. Fletcher, and R. Hardy, 1991: Atlas of Correlative Imaging Anatomy of the Normal Dog: Ultrasound and Computed Tomography, 1st edn. Philadelphia: WB Saunders Co.

Fike, J. R., E. Druy, B. Zook, D. Davis, J. Thompson, E. Chaney, and E. Bradley, 1980: Canine anatomy as assessed by computerized tomography. Am. J. Vet. Res. **41,** 1823–1832.

Girgin, C., A. Sezer, O. Sahin, M. Oder, and C. Dincel, 2007: Giant renal calculus in a solitary functioning kidney. Urol. Int. **78,** 91–92.

Hounsfield, G. N., 1973: Computerized transverse axial scanning (tomography). Br. J. Radiol. **46,** 1016.

Novelline, R. A., J. T. Rhea, and P. Rao, 1999: Helical CT in emergency radiology. Radiology **213,** 321–339.

Ottesen, N., and L. Moe, 1998: An introduction to computed tomography (CT) in the dog. Eur. J. Compan. Anim. Pract. **8,** 29–36.

Ri-Sheng, Y., Z. Wei-Min, and L. Yi-Qing, 2006: CT diagnosis of 52 patients with lymphoma in abdominal lymph nodes. World J. Gastroenterol. **28,** 7869–7873.

Rivero, M. A., J. A. Ramírez, J. M. Vázquez, F. Gil, G. Ramírez, and A. Arencibia, 2005: Normal anatomical imaging of the thorax in three dogs: computed tomography and macroscopic cross sections with vascular injection. Anat. Histol. Embryol. **34,** 215–219.

Ruberte, J., J. Sautet, M. Navarro, A. Carretero, M. Manesse, and F. J. Pérez-Aparicio, 1998: Atlas de Anatomía del perro y del gato: Vol. 3: Abdomen, pelvis y miembro pelviano. Sant Cugat del Vallès, Barcelona: Ed. Multimédica.

Samii, V., D. Biller, and P. Koblik, 1998: Normal cross-sectional anatomy of the feline thorax and abdomen: comparison of computed tomography and cadaver anatomy. Vet. Radiol. Ultrasound. **39,** 504–511.

Schaller, O., 1992: Illustrated Veterinary Anatomical Nomenclature. Stuttgart: Ferdinand Enke Verlag.

Schwartz, S. A., M. S. Taljanovic, S. Smyth, M. J. O'Brien, and L. F. Rogers, 2007: CT findings of rupture, impending rupture, and contained rupture of abdominal aortic aneurysms. Am. J. Roentgenol. **188,** W57–W62.

Schwarz, T., 2003: General Principles for Interpreting CT Studies. The European Association of Veterinary Diagnostic Imaging Yearbook 2003. Glasgow: EAVDI.

Smallwood, J. E., and T. F. George, 1993: Anatomic atlas for computed tomography in the mesaticephalic dog: thorax and cranial abdomen. Vet. Radiol. Ultrasound. **34,** 65–83.

Stickle, R., and J. Hathcock, 1993: Interpretation of computed tomographic images. Vet. Clin. North Am. Small Anim. Pract. **23,** 417–435.

Syed, M. A., T. K. Kim, and H. J. Jang, 2007: Portal and hepatic vein thrombosis in liver abscess: CT findings. Eur. J. Radiol. **61,** 513–519.

Teixeira, M., F. Gil, J. M. Vázquez, L. Cardoso, A. Arencibia, G. Ramírez-Zarzosa, and A. Agut, 2007: Helical computed tomographic anatomy of the canine abdomen. Vet. J. **174,** 133–138.

Thrall, D. E., 1994: Textbook of Veterinary Diagnostic Radiology. Philadelphia: WB Saunders Co.

Vázquez, J. M., G. Ramírez, F. Gil, R. Latorre, F. Moreno, O. López, M. Orenes, and A. Arencibia, 2000: Atlas de Anatomía Clínica. Perro y gato. Cavidades torácica, abdominal y pelviana, 1st edn. Murcia: AG Novograf SA.